Augmented collisional ionization via excited states in XUV cluster interactions



2011 J. Phys. B: At. Mol. Opt. Phys. 44 165102

(http://iopscience.iop.org/0953-4075/44/16/165102)

J. Phys. B: At. Mol. Opt. Phys. **44** (2011) 165102 (5pp) doi:10.1088/0953-4075/44/16/165102

# Augmented collisional ionization via excited states in XUV cluster interactions

**Edward Ackad, Nicolas Bigaouette and Lora Ramunno**

Department of Physics, University of Ottawa, Ottawa, Ontario K1N 6N5, Canada

E-mail: Lora.Ramunno@uottawa.ca

Received 9 March 2011, in final form 25 May 2011
Published 25 July 2011
Online at stacks.iop.org/JPhysB/44/165102

**Abstract**

The impact of atomic excited states is investigated via a detailed model of laser–cluster interactions, which is applied to rare gas clusters in intense femtosecond pulses in the extreme ultraviolet (XUV). We investigate a two-step ionization process via excited atomic states, which allows the creation of high charge states and rapid dissemination of laser energy. Through simulations corresponding to recent argon cluster–XUV experiments, this two-step process is shown to play a primary role; this is consistent with our hypothesis that XUV–cluster interactions provide a unique window into the role of excited states due to the relative lack of photoionization and laser field-driven phenomena. Our analysis suggests that excited states may be important for material interactions with intense radiation in a variety of wavelength regimes, including potential implications for proposed studies of single-molecule imaging with intense x-rays.

(Some figures in this article are in colour only in the electronic version)

Over the last decade, coherent radiation sources have been developed that can probe light–matter interactions at ever smaller wavelengths and unprecedented intensities [1, 2]. Recent experiments have moved into the extreme ultraviolet (XUV), including several that have explored intense XUV interactions with rare gas clusters [3, 4]. The XUV regime near 30 nm is unique because the photon energy is too small for inner shell ionization of rare gas atoms [5], yet too large (at reported intensities) for any appreciable laser-field-driven processes that dominate intense laser–cluster interactions at longer wavelengths, such as collisional heating. We therefore propose that this regime presents a unique opportunity to isolate the influence of the internal electronic structure of atoms within clusters on intense radiation–cluster interactions.

To date, microscopic models of cluster interactions with intense radiation in the near IR [6] or vacuum ultraviolet (VUV) [7–10] have not incorporated effects of excited electronic states of constituent atoms and ions. As a result, its influence in such interactions is unknown over a broad wavelength range, including the XUV.

In this paper, we introduce a general model that explicitly incorporates the effect of atomic and ionic excited states on collisional ionization, and apply it to a molecular dynamics code for rare gas cluster interactions with intense radiation. By including the process whereby a ground-state electron of any charge species can be internally promoted to an excited state by a colliding electron, ionization is allowed to occur through a two-step process: excitation followed by ionization from the excited state. This requires two sequential collisions, each of less energy than is required by single-step collisional ionization from the ground state. This generally applicable two-step process, which we call 'augmented collisional ionization' (ACI), is applied to the 32 nm experiment with argon clusters [3]. ACI is found to dominate, allowing the system to access higher charge states than the single-step collisional ionization process alone.

The incorporation of ACI into our laser–cluster interaction model provides the first explanation of the observation of high charge states ($Ar^{4+}$) in the 32 nm system. Further, we find that cluster atoms quickly become excited and then ionized through ACI, demonstrating that the pulse energy is spread rapidly through the cluster. This work therefore provides a fundamental insight into the dynamics of XUV–cluster interactions, an area that has, to date, been the subject of only a small number of theoretical investigations [3, 4, 11, 12], none of which accounted for the experimentally observed high charge state. A multistep ionization model was proposed that explained the electron spectra for all but the highest pulse intensities [3]. Other theoretical investigations of the electron emission spectra using a kinetic Boltzmann

 

model including non-equilibrium and equilibrium dynamics [11] and using both Monte Carlo and molecular dynamics simulations [12] give possible accounts of the significant low-energy electron yield.

We find that excited states in collisional systems play a crucial role in understanding both the charge state spectrum and how quickly charge states are produced due to increased energy transfer between electrons and ions. Although the XUV provides a unique regime in which to study these effects, our results are more generally applicable. This work thus opens the door to the study of the importance of excited states in other material systems and in wavelength regimes ranging from the infrared to x-rays. Further, the more rapid energy transfer to ions through the ACI process could also affect explosion dynamics, which may be an important consideration in proposed single-molecule imaging studies with intense x-rays [13].

## 1. Method

The motion of the ions and electrons is calculated via classical molecular dynamics. Quantum effects are included by determining transition cross-sections and using a Monte Carlo scheme to determine when excitation or ionization occurs. In the case of ionization, a free electron is added to the dynamics simulation. The new electron's total energy with respect to the outer ionization threshold is dependent on the local field and thus its radial position in the cluster. In the case of excitation, no new electron is added, but the parent atom/ion is set to be in an excited state, which determines its future ionization potential and cross-section.

The photoionization probability is calculated at each time-iteration for every atom and singly charged ion, and this is used to determine if a photoionization event is to occur. The photon flux is determined via the intensity, which is modulated by the pulse time profile and photon absorption. Since we are interested primarily in the generation of the high charge state, we do not average over the spatial profile of the pulse when determining charge state populations, but rather consider only the peak intensity.

The cross-section for the photoionization of neutral argon was obtained from [14], while those of ionic argon were obtained using Los Alamos atomic physics codes [15].

The atom–electron collision in the cluster environment is modelled as an isolated atom–electron collision in a background cluster potential. This allows the collisional cross-sections for both the ionization and excitation to be calculated using an isolated atom–electron model; we include these cross-sections for up to $Ar^{6+}$.

Single-step collisional ionization cross-sections were calculated using the Lotz formula [16]. The Born plane-wave approximation [17] was used for both excitation and ionization from an excited state, similar to [18]. Computed collisional excitation cross-sections were compared to experimentally measurable excitations to metastable states; our results for neutral argon closely match the experimental results for the metastable part of the $3p^6 \rightarrow 3p^5 4s$ excitation ($^3P_0$ and $^3P_2$) [19].

The subset of excited states used consist of single-electron states with $l < 4$, which are the lowest energy states and thus the most important. Including more excited states adds to the total collisional cross-section, although states near the threshold require almost as much energy as ionization and are thus almost as infrequent. The energy of the excited states and the cross-sections were obtained using the Hartree–Fock implementation of the Cowan code [17]. We found that there is some distortion of these excited states for neutrals next to bare $Ar^{4+}$ ions; however, its effect is negligible since this situation does not occur within the simulations.

The inclusion of excited states does not alter photonionization. This is because photoexcitation away from a resonance is rare as only states of $|\Delta l| = 1$ are accessible. The photon wavelength must also be approximately equal to the transition energy. In electron–atom collisions, in contrast, the electron can transfer any amount of its orbital angular momentum and available kinetic energy.

The influence of the cluster is accounted for by determining the potential $V_p$ at the atom due to all particles farther than the nearest neighbour distance, $R$ (>6.4 Bohr for argon), and approximating it as a constant external potential in the vicinity of the atom. The potential at the atom is reinterpreted as the cluster-free threshold of the atom, similar to [9].

This approximation is justified by considering an atom at $\vec{r} = 0$ that is surrounded by two neighbouring ions on the $z$-axis at $\pm\vec{R}$, representing the nearest neighbours in one orthogonal direction with arbitrary charge states $Z_1$ and $Z_2$; this is easily generalized to include neighbours in other directions. Both neighbours contribute a constant term, $Z/R$, to the Hamiltonian of the atom which merely shifts the threshold. Using first-order perturbation theory, the lowest order correction to the eigenvalue is

$$\Delta E = -\frac{Z_1 + Z_2}{R^3} \langle \phi_0 | \hat{q} | \phi_0 \rangle , \qquad (1)$$

where $\hat{q}$ is the quadrupole operator. The state $\phi_0$ is an eigenstate of the atomic Hamiltonian, and therefore the angular momentum operator, making the dipole term zero. The potential of the electrons within $R/2$ of the atom is also removed from $V_p$. The collisional system therefore closely approximates an isolated system as the error is primarily quadrupole.

The screening effects of the electrons within $R/2$ on the ionization potential are not easily modelled microscopically due to the highly collisional nature of the system. Screening effects, if present, would only alter the relative energy of the steps for excitation and ionization, but the energy steps for ACI would still be significantly smaller than those for single-step ionization. Thus this would not change the relative importance of ACI over single-step ionization.

During a collision, the energetically accessible states are determined by the kinetic energy of the impacting electron relative to the target atom's cluster-free threshold. This includes ionization if energetically permissible. The total cross-section for all of the possible final states is used to determine if any excitation or ionization event will occur. If the electron's impact parameter, $b = |\vec{v} \times \vec{r}|/|\vec{v}|$, is within this

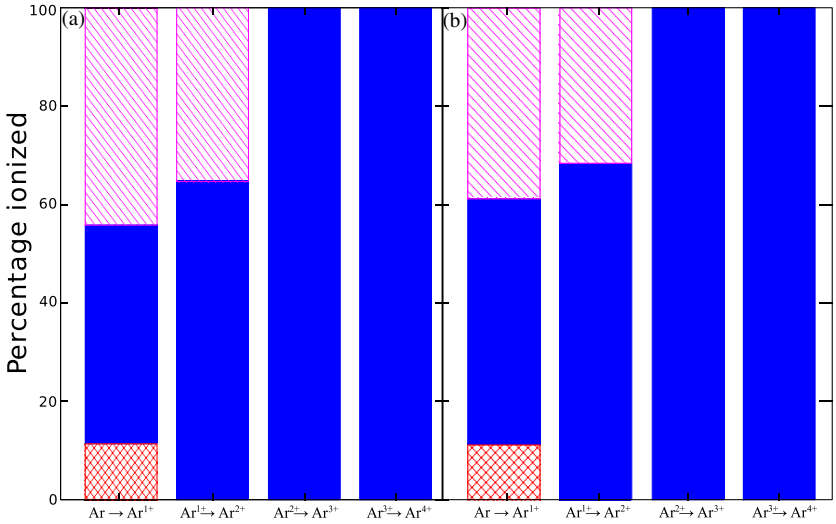


**Figure 1.** The relative contributions of photoionization (diagonal lines), single-step ionization (cross-hatching) and ACI (solid) in the creation of each ion species of argon by the interaction of (a) $Ar_{80}$ and (b) $Ar_{147}$ with 32.8 nm radiation at $5 \times 10^{13}$ W cm$^{-2}$.

total cross-section, then a state is chosen at random, weighted by its cross-section relative to the total cross-section.

We have not included mechanisms for excited state decay. While it is possible for the excited states to decay radiatively, the shortest lived states will be the states of $|\Delta l| = 1$. These decays are on the nanosecond scale [20, 21], thus unlikely to affect our results.

Collisional de-excitation, which entails an impact electron gaining energy by de-exciting the atom, is more probable though still unlikely to play a role. This is because the cross-section for ionization from an excited state is much larger than the de-excitation cross-section, favouring ionization provided the impact electron has the small amount of energy needed to ionize. Further, even if we were to allow collisional de-excitation to occur, it would be unlikely to significantly alter our results, since any impact electron that would gain energy would more than likely use that extra energy to excite or ionize another atom, leading to the same results, on average.

## 2. Results

We simulated the interaction of argon clusters exposed to 32.8 nm radiation both with and without the ACI mechanism included. Conventional collisional ionization was included in all simulations. We used a pulse width of 25 fs and varied the intensity from $5 \times 10^{13}$ to $10^{14}$ W cm$^{-2}$. Although the average cluster size in [3] was 80 atoms, a population of larger clusters is possible in the cluster jet. Thus we considered two sizes: $Ar_{80}$ and the closed-shell icosahedral structure $Ar_{147}$. The smaller closed-shell icosahedral $Ar_{55}$ may also be present but would likely have a much smaller contribution to the $Ar^{4+}$ signal. For each parameter set, we performed $10^4$ simulations. We ran each $Ar_{80}$ simulation to 800 fs and each $Ar_{147}$ simulation to 1 ps.

In table 1, we list the average yield of $Ar^{4+}$ per cluster for each set of simulations. It shows that $Ar^{4+}$ emerges at the intensity quoted in [3] only when ACI is included. Without ACI, $Ar^{4+}$ do occur at higher intensities, though the yield is orders of magnitude less than when ACI is included. While we see an increase in the number of $Ar^{4+}$ in the larger versus smaller clusters, the influence of cluster size is still smaller than the increase from the ACI ionization channel. Thus we find that, at all intensities, ACI is the single largest effect.

**Table 1.** Average yield of $Ar^{4+}$ at different intensities for argon cluster sizes of 80 and 147, with (third column) and without (second column) ACI included.

| | ACI | |
|---|---|---|
| Intensity (W cm$^{-2}$) | No | Yes |
| $Ar_{80}$ | | |
| $5 \times 10^{13}$ | 0 | 0.0114 |
| $7.5 \times 10^{13}$ | 0.0002 | 0.0601 |
| $10 \times 10^{13}$ | 0.0008 | 0.1490 |
| $Ar_{147}$ | | |
| $5 \times 10^{13}$ | 0 | 0.0338 |
| $7.5 \times 10^{13}$ | 0.0008 | 0.1510 |
| $10 \times 10^{13}$ | 0.0037 | 0.4183 |

To further illustrate the dominance of ACI, figure 1 plots that fraction of each ionization channel that led to the creation of the various charge states: photoionization is represented by diagonal line fill, ACI by solid fill and single-step collisional ionization by cross-hatch fill. The left histogram is for $Ar_{80}$, and the right for $Ar_{147}$. Photoionization contributes only to the creation of $Ar^{1+}$ and $Ar^{2+}$, as expected. Since the percentage of photoionization is lower in the larger cluster, we see that clusters become more collisional as their size increases. Single-step collisional ionization contributes significantly only to the creation of $Ar^{1+}$. ACI, however, dominates the creation of $Ar^{2+}$ to $Ar^{4+}$, and is the exclusive mechanism for the creation of $Ar^{4+}$.

Next, we examine the dynamics of the interaction to further explore the role of ACI and the prevalence of the excited

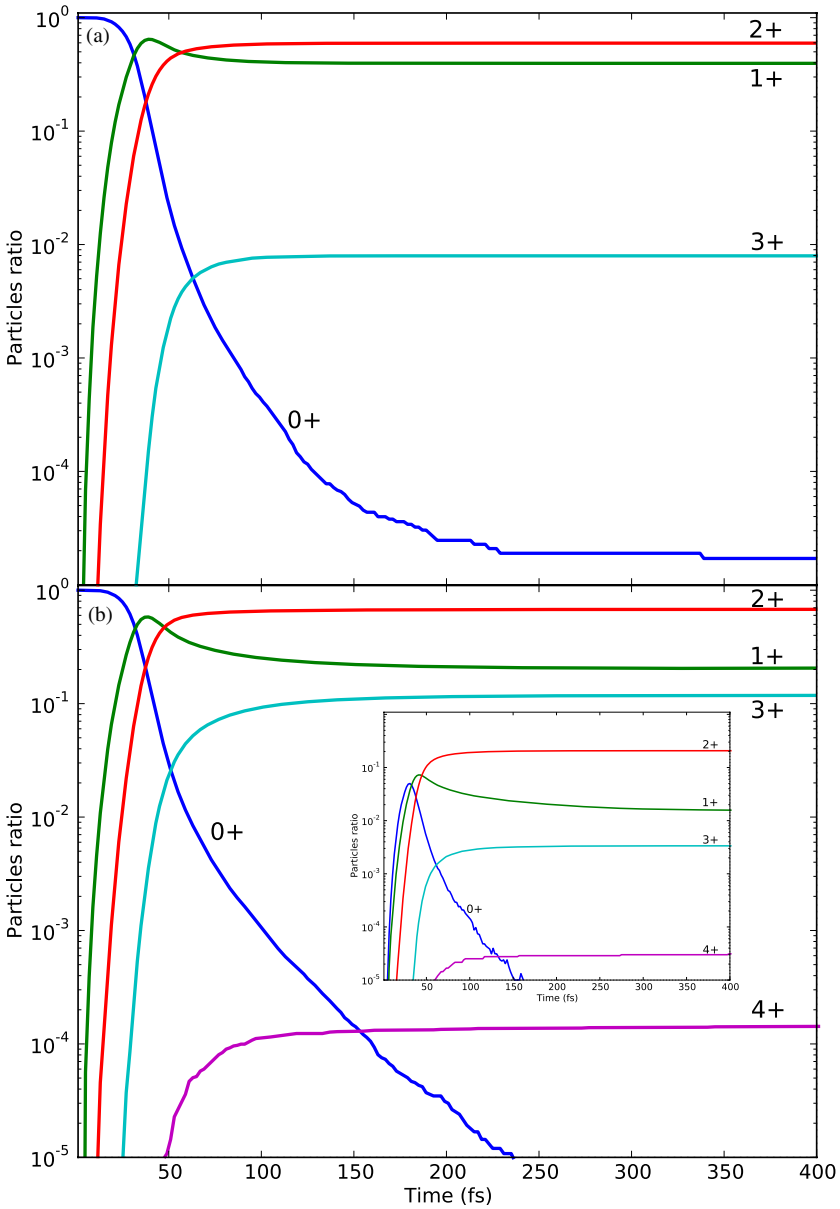


**Figure 2.** The (normalized) charge species populations versus time for $Ar_{80}$ interaction with 32.8 nm radiation, without (a) and with (b) ACI. The inset in (b) gives the relative excited charge species population versus time.

states. Figure 2 plots the relative (inner ionized) charge state population versus time for $Ar_{80}$ both without (top) and with (bottom) ACI included for a 25 fs laser pulse which starts at the origin and peaks at around 34 fs. With ACI, the higher charge states appear earlier and in greater abundance. The peak in $Ar^{1+}$ happens roughly 2 fs earlier with ACI, the $Ar^{2+}$ surpasses $Ar^{1+}$ 10 fs earlier and a sizable $Ar^{3+}$ population emerges 7 fs earlier and surpasses the atomic population around 12 fs earlier than without ACI. The final abundance of $Ar^{3+}$ is more than an order of magnitude larger when ACI is present. In both cases, the $Ar^{2+}$ is the most abundant species at the end, but the ratios between species populations are very different. With ACI we also see the emergence of $Ar^{4+}$, which appears at the tail of the laser pulse but reaches a plateau around 100 fs later, at which time it surpasses the abundance of atoms.

The shapes of the curves in figure 2 can be understood by regarding the ensemble results in terms of a rate equation model in which population flows from neutral atoms to the higher charge states by ionization couplings. We find that the neutral population decreases rapidly only once the laser has approached its peak. Afterwards population largely flows to the ion charge states by a mix of further photoionization (minor) and collisional ionization (dominant). The earlier crossings mentioned above and the larger populations of $Ar^{2+}$, $Ar^{3+}$ and $Ar^{4+}$ obtained in figure 2(b) are due to the increased coupling of the different ion charge states by allowing for the collisional excitation step and ACI. In both cases there continues to be a decrease in the $Ar^{1+}$ population after the laser pulse due to collisions, although the decrease is much larger when ACI is included.

The inset in figure 2 displays the fraction of each charge species that is in excited states as a function of time. The abundance of excited states (after the pulse peak) closely follows that of the internal charge states; a sizable fraction of each charge species is excited. Most ions remain excited for less than a few femtoseconds due to being ionized via collisions with previously ionized cluster-bound electrons.

Figure 1 shows that virtually all $Ar^{3+}$ and $Ar^{4+}$ are ionized by ACI. Figure 2 shows that these populations grow significantly once the laser pulse is finished (as they are due to ACI) and that these collisional processes are still frequent after the laser.

ACI thus allows the cluster to reach high charges and to do so earlier than otherwise possible. This is a result of having a significant proportion of each charge species excited. Consequently, impact electrons do not require as much kinetic energy to ionize the excited electrons as single-step ionization or as the excitation step itself. The final charge state spectra indicated in figure 2 were generated by runs at a single intensity, which would represent only the peak region of the laser pulse.

## 3. Conclusion

In summary, we found that the detection of $Ar^{4+}$ in [3] can be explained by augmented collisional ionization (ACI), a two-step process wherein collisional ionization occurs via intermediate excited states. ACI was found to dominate; it occurs much more frequently than single-step collisional ionization from the ground state which alone cannot reproduce the high charge state. While we applied our model to cluster–XUV interactions, ACI will likely play a role in any highly collisional system, including in a variety of finite condensed systems interacting with intense radiation in a wide range of wavelength regimes.

We have also shown that ACI provides a route to high charge states in a shorter time, due to the efficacy of the energy transfer afforded by the lower energy gaps of excitation compared to direct ionization. The energy imparted to a small finite system will thus be highly sensitive to the ramp up of the pulse, which may have consequences for the direct imaging of single biomolecules with short, intense x-ray pulses. Thus a good understanding of the excited states of the photo-sensitive parts of the biomolecule (i.e. atoms and molecules that have largest photoionization cross-sections) and a sharp ramp up of the imaging pulse will be crucial.

## Acknowledgments

The authors would like to thank Thomas Brabec, Paul Corkum and Jean-Paul Britcha for many fruitful discussions. This work is supported by NSERC, MRI and CFI.

## References

[1] Wabnitz H *et al* 2002 Multiple ionization of atom clusters by intense soft x-rays from a free-electron laser *Nature* **420** 482
[2] Young L *et al* 2010 Femtosecond electronic response of atoms to ultra-intense x-rays *Nature* **466** 56
[3] Bostedt C *et al* 2008 Multistep ionization of argon clusters in intense femtosecond extreme ultraviolet pulses *Phys. Rev. Lett.* **100** 133401
[4] Murphy B F, Hoffmann K, Belolipetski A, Keto J and Ditmire T 2008 Explosion of xenon clusters driven by intense femtosecond pulses of extreme ultraviolet light *Phys. Rev. Lett.* **101** 203401
[5] Gnodtke C, Saalmann U and Rost J M 2009 Ionization and charge migration through strong internal fields in clusters exposed to intense x-ray pulses *Phys. Rev.* A **79** 041201
[6] Fennel Th *et al* 2010 Laser-driven nonlinear cluster dynamics *Rev. Mod. Phys.* **82** 1793–842
[7] Siedschlag C and Rost J-M 2004 Small rare-gas clusters in soft x-ray pulses *Phys. Rev. Lett.* **93** 043402
[8] Santra R and Greene C H 2003 Xenon clusters in intense VUV laser fields *Phys. Rev. Lett.* **91** 233401
[9] Fennel T, Ramunno L and Brabec T 2007 Highly charged ions from laser–cluster interactions: local-field-enhanced impact ionization and frustrated electron-ion recombination *Phys. Rev. Lett.* **99** 233401
[10] Jungreuthmayer C, Ramunno L, Zanghellini J and Brabec T 2005 Intense VUV laser cluster interaction in the strong coupling regime *J. Phys. B: At. Mol. Opt. Phys.* **38** 3029–36
[11] Ziaja B, Wabnitz H, Weckert E and Möller T 2008 Femtosecond non-equilibrium dynamics of clusters irradiated with short intense VUV pulses *New J. Phys.* **10** 043003
[12] Arbeiter M and Fennel T 2010 Ionization heating in rare-gas clusters under intense XUV laser pulses *Phys. Rev.* A **82** 013201
[13] Chapman H N 2009 X-ray imaging beyond the limits *Nat. Mater.* **8** 299
[14] Marr G V and West J B 1976 Absolute photoionization cross-section tables for helium, neon, argon, and krypton in the VUV spectral regions *Atomic Data Nucl. Data Tables* **18** 497
[15] Archer B J, Clark R E H, Fontes C J and Zhang H 2000 Gipper user manual *LA-UR-00-5693*
[16] Lotz W 1967 An empirical formula for the electron-impact ionization cross-section *Z. Phys.* A **206** 205
[17] Cowan R D 1981 *The Theory of Atomic Structure and Spectra* (Berkeley, CA: University of California Press)
[18] Micheau S, Bonte C, Dorchies F, Fourment C, Harmand M, Jouin H, Peyrusse O, Pons B and Santos J 2007 Dynamics of rare gas nanoclusters irradiated by short and intense laser pulses *High Energy Density Phys.* **3** 191–7
[19] Borst W L 1974 Excitation of metastable argon and helium atoms by electron impact *Phys. Rev.* A **9** 1195–200
[20] Bruce M R, Layne W B, Whitehead C A and Keto J W 1990 Radiative lifetimes and collisional deactivation of two-photon excited xenon in argon and xenon *J. Chem. Phys.* **92** 2917–26
[21] Eichhorn C, Fritzsche S, Löhle S, Knapp A and Auweter-Kurtz M 2009 Time-resolved fluorescence spectroscopy of two-photon laser-excited 8p, 9p, 5f, and 6f levels in neutral xenon *Phys. Rev.* E **80** 026401